

## Lithium cluster anions: Photoelectron spectroscopy and ab initio calculations

Anastassia N. Alexandrova, Alexander I. Boldyrev, Xiang Li, Harry W. Sarkas, Jay H. Hendricks et al.

Citation: *J. Chem. Phys.* **134**, 044322 (2011); doi: 10.1063/1.3532832

View online: <http://dx.doi.org/10.1063/1.3532832>

View Table of Contents: <http://jcp.aip.org/resource/1/JCPSA6/v134/i4>

Published by the AIP Publishing LLC.

---

### Additional information on J. Chem. Phys.

Journal Homepage: <http://jcp.aip.org/>

Journal Information: [http://jcp.aip.org/about/about\\_the\\_journal](http://jcp.aip.org/about/about_the_journal)

Top downloads: [http://jcp.aip.org/features/most\\_downloaded](http://jcp.aip.org/features/most_downloaded)

Information for Authors: <http://jcp.aip.org/authors>

## ADVERTISEMENT

**SHARPEN YOUR  
COMPUTATIONAL  
SKILLS.**



Subscribe for  
**\$49** | year



**computing**  
in **SCIENCE & ENGINEERING**

Scientific  
Computing  
with GPUs

# Lithium cluster anions: Photoelectron spectroscopy and *ab initio* calculations

Anastassia N. Alexandrova,<sup>1,a)</sup> Alexander I. Boldyrev,<sup>2,a)</sup> Xiang Li,<sup>3</sup> Harry W. Sarkas,<sup>3</sup> Jay H. Hendricks,<sup>3</sup> Susan T. Arnold,<sup>3</sup> and Kit H. Bowen<sup>3,a)</sup>

<sup>1</sup>*Department of Chemistry and Biochemistry, University of California, Los Angeles, California 90095-1569, USA*

<sup>2</sup>*Department of Chemistry and Biochemistry, Utah State University, Logan, Utah 84322, USA*

<sup>3</sup>*Departments of Chemistry and Materials Science, Johns Hopkins University, Baltimore, Maryland 21218, USA*

(Received 7 October 2010; accepted 4 December 2010; published online 31 January 2011)

Structural and energetic properties of small, deceptively simple anionic clusters of lithium,  $\text{Li}_n^-$ ,  $n = 3-7$ , were determined using a combination of anion photoelectron spectroscopy and *ab initio* calculations. The most stable isomers of each of these anions, the ones most likely to contribute to the photoelectron spectra, were found using the gradient embedded genetic algorithm program. Subsequently, state-of-the-art *ab initio* techniques, including time-dependent density functional theory, coupled cluster, and multireference configurational interactions methods, were employed to interpret the experimental spectra. © 2011 American Institute of Physics. [doi:10.1063/1.3532832]

## I. INTRODUCTION

Lithium cluster anions are deceptively simple. They, in fact, represent a challenge for both experimental and theoretical characterizations. Having small masses, lithium cluster anions acquire high speeds and are difficult to decelerate in photoelectron spectroscopic experiments. In addition, preventing lithium from oxidizing requires an unusually clean vacuum environment and delicate sample preparation. On the theoretical side, the highly diffusive nature of the bound electron and the multiconfigurational nature of the wavefunctions of the neutral clusters lead to numerous complications, making results sensitive to the choice for computational methodology and basis sets. These characteristics make the anions addressed in the present study an especially challenging case, as was brought up in recent reviews on anions, including cluster anions.<sup>1-3</sup> Thus, it is not surprising that there are only a few reported studies on anionic lithium clusters.<sup>4-15</sup>

Among these,  $\text{Li}_2^-$  has received the most attention, but even in this case, peculiarities in its electronic structure can be seen.<sup>4-10</sup> Studies of larger lithium cluster anions have been fewer.<sup>10-14</sup> Photoelectron spectra of alkali tetramers were reported in 1995.<sup>11</sup> It was observed that  $\text{Li}_4^-$  has an anomalous photoelectron spectrum as compared to all other alkali tetramers.<sup>11</sup>  $\text{Li}_4^-$  was also studied theoretically.<sup>10</sup>  $\text{Li}_6^{+1/0/-1}$  were investigated via high level *ab initio* calculations.<sup>12</sup> Atomization and ionization energies were computed.  $\text{Li}_6^-$  was shown to have a tetragonal bipyramid ( $D_{4h}$ ) symmetry. This work also demonstrated that the computed properties of lithium clusters are very sensitive to the theoretical method and basis set used. Density functional theory (DFT) and high level *ab initio* calculations of  $\text{Li}_7^-$  predicted that these species have three low-energy isomers: a  $D_{5h}$  structure and two dif-

ferent  $C_{3v}$  structures.<sup>13</sup> A systematic unbiased search for the global minimum of  $\text{Li}_x^{-1/0/+1}$  ( $x = 5-7$ ) was done by Alexandrova and Boldyrev.<sup>14</sup> The chemical bonding in these clusters was then thoroughly investigated, and it was demonstrated that multiple aromaticity and antiaromaticity present in these clusters can explain their global minimum shapes.<sup>14</sup> Large cluster anions and their electronic structure were also studied experimentally by Roux and Bowen.<sup>15</sup>

Overall, there are many missing pieces in our understanding of lithium cluster anions. The present work is intended to clarify this incomplete picture. We report the results of the systematic joint theoretical and photoelectron spectroscopic study of the  $\text{Li}_x^-$  ( $x = 3-7$ ) clusters. Lithium cluster anions were generated in the gas phase and their photoelectron spectra recorded. Cluster geometries were identified theoretically. Vertical electron detachment energies were calculated and compared to the experiment.

## II. EXPERIMENTAL METHODS

Negative ion photoelectron spectroscopy is conducted by crossing a mass-selected beam of negative ions with a fixed frequency photon source and energy analyzing the resultant photodetached electrons. This technique is governed by the energy-conserving relationship  $h\nu = \text{EKE} + \text{EBE}$ , where  $h\nu$  is the photon energy, EKE is the measured electron kinetic energy, and EBE is the electron binding energy.

Two different types of anion photoelectron spectrometers were used to study the lithium cluster anions. For  $\text{Li}_{1-4}^-$ , they were produced in a high temperature, supersonic expansion ion source. In this source lithium metal is heated to 1300 K, yielding  $\sim 50$  Torr of lithium vapor which was coexpanded with 50–150 Torr of high purity argon into high vacuum through a 0.15 mm nozzle. A negatively biased hot filament injected low-energy electrons directly into the expanding jet in the presence of a predominantly axial magnetic field,

<sup>a)</sup>Authors to whom correspondence should be addressed. Electronic addresses: ana@chem.ucla.edu, a.i.boldyrev@aggiemail.usu.edu, and kbowen@jhu.edu.

generating negative ions. The resultant beam was skimmed by a heated skimmer, and anions were transported through a series of ion optical components through an  $\mathbf{E} \times \mathbf{B}$  Wien filter, which served as a mass selector. The mass-selected cluster anion beam was then crossed with the intracavity beam of an argon ion laser. A small solid angle of the resulting photodetached electrons was accepted into a hemispherical electron energy analyzer, where they were energy analyzed and counted. Photoelectron spectra were recorded at an instrumental resolution of 30 meV, using 110–120 circulating watts of 2.540 eV photons.

For  $\text{Li}_{4-7}^-$  cluster anions, they were generated in a laser vaporization source in which 2.331 eV photons from a Nd:YAG laser struck a rotating, translating lithium rod. No inert carrier gas was used. This resulted in lithium cluster anions, uncontaminated by impurities such as oxides. Mass analysis and selection were accomplished with a linear time-of-flight mass spectrometer, a second Nd:YAG laser was used for photodetachment, and a magnetic bottle was utilized for electron energy analysis. The photoelectron spectra of the anions reported here were measured with 3.493 eV photons.

### III. THEORETICAL METHODS

The global minimum structures of the clusters containing five to seven atoms discussed herein can be found in our previous work.<sup>14</sup> The global minimum of  $\text{Li}_3^-$  was identified manually within the present study. The global minimum of  $\text{Li}_4^-$  was identified using the same protocol as in Ref. 14. Namely, the gradient embedded genetic algorithm (GEGA) program<sup>16</sup> was used for the search. The details of the GEGA procedure were reported elsewhere.<sup>14,16</sup> The search was performed using a hybrid density functional method including a mixture of Hartree–Fock exchange with density functional exchange–correlation potentials (B3LYP) (Refs. 17–19) and a small split-valence basis set (3-21G).<sup>20,21</sup> The predicted structures of the global and stable local minima were further refined at higher levels of theory. We first used B3LYP with a larger basis set (6-311++G\*\*) for geometry optimization and vibrational frequency analysis. In addition, the geometries and vibrational frequencies were obtained using the coupled cluster method with single and double excitations and triple excitation treated noniteratively, CCSD(T)/6-311+G\*.<sup>22–28</sup> All relative energies were zero point energy corrected. The B3LYP geometries were used for the further calculations of the photoelectron spectra using the time-dependent density functional theory with an extended basis set [TD-B3LYP/6-311+G(df)].<sup>29,30</sup> In the latter approach, for the singlet  $\text{Li}_x^-$  anions, the first vertical detachment energy (VDE) was calculated at B3LYP as the lowest transition from the ground singlet state of the anion into the final lowest doublet state of the neutral  $\text{Li}_x$  species at the geometry optimized for the anion. Then, the vertical excitation energies of the neutral species (at the TD-B3LYP level) were added to the first VDE to obtain the second and higher VDEs. For the doublet ground state of  $\text{Li}_x^-$ , the first two VDEs were calculated at the B3LYP level of theory as the lowest transition from the doublet ground state of the anion into the final lowest singlet and triplet states of the

neutral species at the geometry optimized for the anion. Then the vertical excitation energies of the neutral species (at the TD-B3LYP level) calculated for the singlet and triplet states added to the two lowest VDEs with the singlet and triplet final states, respectively, to obtain the second and higher VDEs. The CCSD(T) geometries were used for all other calculations of electron detachment energies. Theoretical VDEs were further obtained at the UCCSD(T)/6-311+G(2df) level and also RCCSD(T)/6-311+G(2df) in combination with the equation of motion (EOM) protocol. The outer valence Green function method [R(U)OVGF/6-311+G(2df)] (Refs. 31–34) was also used. In addition, the multireference CASSCF-MRCISD/6-311+G(2df) (Refs. 35 and 36) calculations were done for the smallest,  $\text{Li}_3^-$ , cluster.

Calculations were done using GAUSSIAN 03 (Ref. 37) (B3LYP, TD-B3LYP, OVGF, and CCSD(T) calculations) and MOLPRO 2000.1 (Ref. 38) (EOM-CCSD(T), and CASSCF-MRCI). MOLDEN (Ref. 39) and GAUSSVIEW 3.09 were used for structure and MO visualization, respectively.

### IV. EXPERIMENTAL RESULTS

The photoelectron spectra of  $\text{Li}_{1-7}^-$  are shown in Fig. 1. Photodetachment transitions occur between the ground state of an anion and the ground and excited states of its neutral counterpart, the latter being at the structure of the anion. The profile of the transition is governed by the Franck–Condon overlap between the two. The EBE value at the intensity maximum in the Franck–Condon profile is the VDE.

A single, sharp peak is observed in the spectrum of  $\text{Li}_1^-$ , the maximum of which occurs at an EBE of 0.62 eV. This reproduces the well known electron affinity of the lithium atom. For  $\text{Li}_2^-$ , three transitions are observed at EBE = 0.53, 1.55, and 2.18 eV, and for  $\text{Li}_3^-$ , two transitions are seen at EBE = 1.30 and 2.0 eV. The two spectra shown for  $\text{Li}_4^-$  were recorded on two different apparatus, each using a different type of cluster anion source. The  $\text{Li}_4^-$ , whose spectrum is shown as an inset in Fig. 1, was produced in an oven-based source, and it exhibits two relatively sharp transitions at EBE = 0.76 and 0.85 eV. The other  $\text{Li}_4^-$  spectrum, however, was taken with  $\text{Li}_4^-$ , which was produced using the laser vaporization source. It exhibits a broadband whose maximum occurs around an EBE of ~2.1 eV. The spectra of  $\text{Li}_5^-$ ,  $\text{Li}_6^-$ , and  $\text{Li}_7^-$  show some similarities. In each case, there is a broad, partially structured band between 1 and 2 eV and another transition region between 2.2 and 2.5 eV, although these features shift slightly toward higher EBE with increasing cluster size. The spectrum of  $\text{Li}_7^-$ , however, stands out due to its relatively structured character, with transitions occurring at EBEs of 1.25, 1.58, 1.89, and 2.45 eV.

### V. THEORETICAL RESULTS AND DISCUSSION

Figure 2 shows the structures of the global minima of the  $\text{Li}_x^-$ ,  $x = 3-7$  clusters as found by GEGA and refined at the CCSD(T)/6-311+G\* level of theory. The valence molecular orbitals of the clusters are given in Fig. 3.

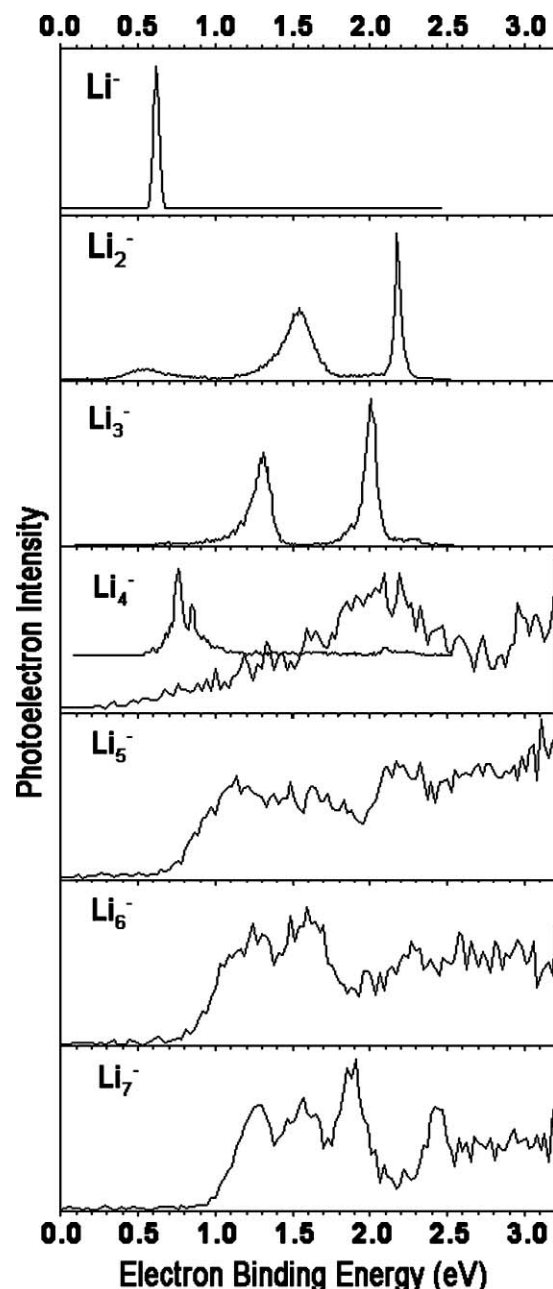


FIG. 1. Experimental anion photoelectron spectra of lithium cluster anions,  $\text{Li}_x^-$ ,  $x = 1-7$ .

### A. $\text{Li}^-$ and $\text{Li}_2^-$

We used  $\text{Li}^-$  and  $\text{Li}_2^-$  anions as test probes of our theoretical methods. For  $\text{Li}^-$ , we calculated the following EBE values at various levels of theory: 0.558 eV [B3LYP/6-311+G(2df)], 0.511 eV (ROVGF/6-311+G(2df) with the pole-strength being 0.70, and 0.613 eV [UCCSD(T)/6-311+G(2df)], which can be compared with the previous experimentally measured value of 0.6180(5) eV as well as with the result of the measurement in this study.<sup>40</sup> One can see that EBE calculated at the CCSD(T)/6-311+G(2df) level of theory is quite accurate, while at B3LYP/6-311+G(2df) it is off by 0.06 eV. The ROVGF/6-311+G(2df) method failed because the pole-strength is too low (it should be more than 0.8).

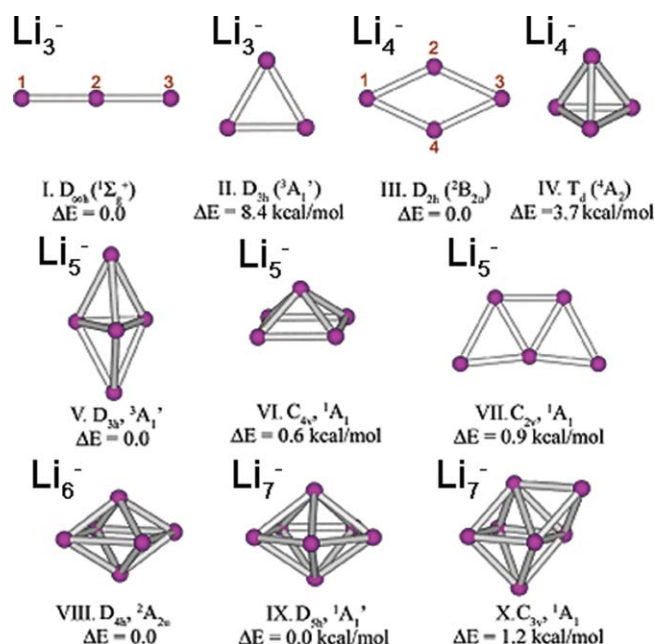


FIG. 2. Lowest-energy structures of  $\text{Li}_x^-$  clusters (CCSD(T)/6-311+G(2df)//CCSD(T)/6-311+G\*+ZPE/CCSD(T)/6-311+G\* level of theory).

In the case of  $\text{Li}_2^-$ , the calculated values  $r_e = 3.027 \text{ \AA}$  and  $\omega_e = 226 \text{ cm}^{-1}$  (B3LYP/6-311+G\*) and  $r_e = 3.064 \text{ \AA}$  and  $\omega_e = 228 \text{ cm}^{-1}$  are in a good agreement with the experimental results of Sarkas *et al.*,<sup>4</sup> i.e.,  $r_e = 3.094 \pm 0.015 \text{ \AA}$  and  $\omega_e = 232 \pm 35 \text{ cm}^{-1}$ . For  $\text{Li}_2^-$ , we calculated that the VDE of the lowest EBE peak, corresponding to the  $^1\Sigma_g^+$  ( $1\sigma_g^2$ ) final electronic state, is 0.50 eV [B3LYP/6-311+G(2df)], 0.73 eV (ROVGF/6-311+G(2df) with the pole-strength being 0.94, and 0.49 eV [UCCSD(T)/6-311+G(2df)], which can be compared with our experimental value, 0.53 eV.<sup>1</sup> For the VDE of the next higher EBE peak, corresponding to the  $^3\Sigma_u^+$  ( $1\sigma_g^1 1\sigma_u^1$ ) final electronic state, we calculated it to be 1.39 eV [B3LYP/6-311+G(2df)], 1.49 eV (ROVGF/6-311+G(2df) with the pole-strength being 0.94, and 1.51 eV [UCCSD(T)/6-311+G(2df)], which can be compared with our experimental value of 1.55 eV.<sup>4</sup> Finally, for the VDE of the third highest EBE peak, corresponding to the  $^1\Sigma_u^+$  ( $1\sigma_g^1 1\sigma_u^1$ ) final electronic state, we calculated 2.37 eV [B3LYP/6-311+G(2df)], which can be compared with our experimental value of 2.18 eV.<sup>4</sup> Again, for the first two peaks, the CCSD(T)/6-311+G(2df) method gives the best agreement with the experiment.

### B. $\text{Li}_3^-$

The linear, singlet structure ( $D_{\infty h}$ ,  $^1\Sigma_g^+$ ) (species I in Fig. 2) is the global minimum for  $\text{Li}_3^-$ , in agreement with an earlier report.<sup>10</sup> The low-lying triplet triangular ( $D_{3h}$ ,  $^3A_2'$ ) isomer II was found to be higher in energy by 5.4 kcal/mol (B3LYP/6-311+G(2df)//B3LYP/6-311+G\*) and 8.4 kcal/mol (CCSD(T)/6-311+G(2df)//CCSD(T)/6-311+G\*). Table SI in supplementary material<sup>41</sup> shows the calculated molecular parameters of these two isomers (results are consistent between B3LYP and CCSD(T) calculations).



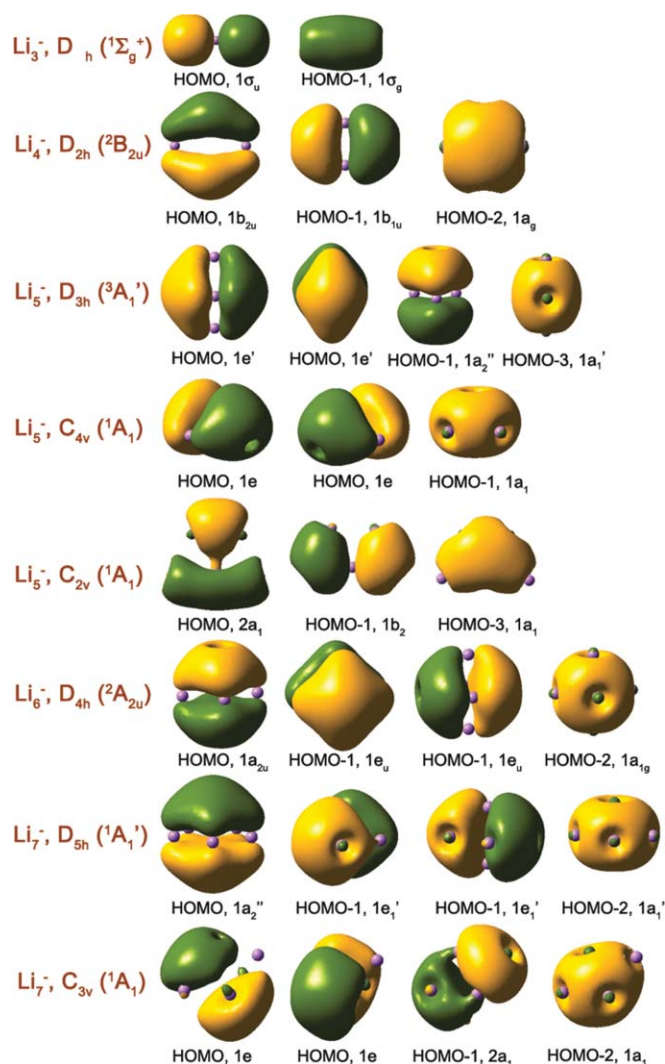


FIG. 3. Valence molecular orbitals of the clusters shown in Fig. 2 (OVGF-order).

Table I shows theoretically evaluated vertical electron detachment energies for species I and II. Overall, for species I, there is a good agreement between VDEs obtained at different levels of theory. However, a trend can be observed in which as electron correlation effects mount, the first VDE exhibits a

blue shift. Compared to the measured VDE of 1.30 eV, the most accurate results come from the CASSCF-MRCI calculations (last column in Table I) which calculate the first VDE to be 1.29 eV. The feature corresponds to the detachment of an electron from the HOMO ( $1\sigma_u$ ), a  $\sigma$ -orbital with a nodal plane running through the central Li atom (see Fig. 3 for the picture of the molecular orbitals of this cluster). The second VDE in the spectrum is predicted to be around 1.94 eV, although a slight inconsistency is also observed among theoretical methods. Theory underestimates the value according to the experimental result of 2.20 eV. The corresponding electron detachment happens from the HOMO-1 ( $1\sigma_g$ ), a completely bonding MO (Fig. 3). The II ( $D_{3h}$ ,  $^3A_2'$ ) isomer is not present under our experimental conditions, i.e., there is no peak at 0.73 eV (CCSD(T)/6-311+G(2df)/CCSD(T)/6-311+G\*) in the experimental spectrum. That is consistent with its high relative energy 8.4 kcal/mol at CCSD(T)/6-311+G(2df)/CCSD(T)/6-311+G\*+ZPE.

### C. $Li_4^-$

$Li_4^-$  is a rhombus structure,  $D_{2h}$  ( $^2B_{2u}$ ) (III in Fig. 2). The GEGA search does not, in general, recognize the symmetry of clusters, so the  $D_{2h}$  symmetry was determined afterward and imposed manually in calculations at higher levels. The ground spectroscopic state was then identified. Table SII (Ref. 41) contains the computed molecular properties of the cluster, Table II presents its theoretical photoelectron spectrum, and the second row in Fig. 3 contains the MOs of the cluster. The corresponding neutral cluster,  $Li_4$ , is a closed-shell. It was therefore possible to compute the electronic excitation energies for the neutral to the singlet and triplet excited states and to recover the corresponding VDEs using TD-B3LYP method. Overall, there is a good agreement between VDEs obtained at different levels of theory. However, OVGF results consistently stand out by overestimating the VDEs. The high-spin  $Li_4^-$  ( $T_d$ ,  $^4A_2$ ) isomer IV is a minimum [see Table SII (Ref. 41)], but it is 3.7 kcal/mol (B3LYP/6-311+G\*) or 3.8 kcal/mol (UCCSD(T)/6-311+G(2df)/UCCSD(T)/6-311+G\*) higher in energy than the global minimum rhombus isomer.

TABLE I. Calculated photoelectron spectrum of two lowest isomers of  $Li_3^-$ .

MO and final state	VDE (eV)			
	TD-B3LYP/6-311+G(2df)// B3LYP/6-311+G*	RCCSD(T)/6-311+G(2df)// CCSD(T)/6-311+G*	ROVGF/6-311+G(2df)// CCSD(T)/6-311+G*	CASMRCI/6-311+G(2df) (10,16)// CCSD(T)/6-311+G*
$Li_3^-$ ( $D_h$ , $^1\Sigma_g^+$ ), VDE (eV)				
$1\sigma_u$ ( $^2\Sigma_u^+$ )	1.09	1.21	1.23 (0.80) <sup>a</sup>	1.29
$1\sigma_g$ ( $^2\Sigma_g^+$ )	1.98	1.87	1.91 (0.68) <sup>b</sup>	1.94
$Li_3^-$ ( $D_{3h}$ , $^3A_2$ ), VDE (eV)				
$1e'$ ( $^2E'$ )	0.76	0.73	1.12 (0.84)	
$1a_1'1e'^2$ ( $^4A_2'$ )	1.83	1.78	2.91 (0.73) <sup>b</sup>	

<sup>a</sup>Numbers in parentheses represent pole-strengths.

<sup>b</sup>Pole-strength is too low.

TABLE II. Calculated photoelectron spectrum of  $\text{Li}_4^-$  ( $D_{2h}$ ,  $^2B_{2u}$ ), species II.

MO and final state	VDE (eV)			
	TD-B3LYP/6-311+G(2df)// B3LYP/6-311+G*	RCCSD(T)/6-311+G(2df)// CCSD(T)/6-311+G*	UOVGF/6-311+G(2df)// CCSD(T)/6-311+G*	EOM-CCSD(T)/6-311+G(2df)// CCSD(T)/6-311+G*
$1b_{2u}$ ( $^1A_g$ )	0.68	0.61	0.82 (0.89) <sup>a</sup>	0.61
$1b_{1u}$ ( $^3B_{3g}$ )	1.11	1.14	1.26 (0.84)	
$1b_{1u}$ ( $^1B_{3g}$ )	2.02			1.76
$1a_g$ ( $^1B_{2u}$ )	2.43			2.10
$1a_g$ ( $^3B_{2u}$ )	2.48		2.50 (0.72) <sup>b</sup>	

<sup>a</sup>Numbers in parentheses represent pole-strengths.<sup>b</sup>Pole-strength is too low.

The first feature in the spectrum of the  $\text{Li}_4^-$  ( $D_{2h}$ ,  $^2B_{2u}$ ) cluster III corresponds to the electron detachment from the singly occupied HOMO ( $1b_{2u}$ ) (Fig. 3). TD-B3LYP, RCCSD(T), and EOM-CCSDT calculations predict this VDE to be between 0.6 and 0.7 eV, whereas UOVGF slightly overestimates it. The second and third VDEs correspond to the loss of an electron from the HOMO-1 ( $1b_{1u}$ ), resulting in a triplet and singlet final spectroscopic state, respectively. The remaining theoretically predicted features correspond to the electron detachment from the deepest valence MO, the completely bonding HOMO-2 ( $1a_g$ ) (Fig. 3).

The two  $\text{Li}_4^-$  spectra shown in Fig. 1 are inconsistent with each other. Moreover, our calculation also fails to clarify the situation. If the peaks in the spectral inset correspond to the predicted lowest EBE transition around  $\sim 0.7$  eV, then why does it not exhibit the multiple predicted transitions between EBEs of 1.7 and 2.5 eV (see Table II)? Likewise, in the case of the other  $\text{Li}_4^-$  spectrum, where a broad band does cover the 1.7–2.5 eV region of predicted transitions, where is the predicted lowest EBE transition around 0.7 eV? It appears that  $\text{Li}_4^-$  remains an enigma. The spectral inconsistency is probably related to the two different source conditions under which  $\text{Li}_4^-$  was produced. There is the possibility that hydrides or even dihydrides were generated and that these “leaked” into the mass of  $\text{Li}_4^-$ , but the theoretically predicted spectra of such species do not match the observed spectra. Our GEGA searches for the global minimum structures revealed that linear  $\text{LiLiHLiLi}^-$  and  $\text{LiHLiHLiLi}^-$  structures are the global minima for the  $\text{Li}_4\text{H}^-$  and  $\text{Li}_4\text{H}_2^-$  anions. The calculated first and second VDEs of  $\text{LiLiHLiLi}^-$  with the  $^2\Sigma_g^+$  ( $1\sigma_g^2 1\sigma_u^2 2\sigma_g^1$ ) and  $^2\Sigma_u^+$  ( $1\sigma_g^2 1\sigma_u^1 2\sigma_g^2$ ) final states were found to be 1.57 and 1.76 eV, respectively [TD-B3LYP/6-311+G(2df)]. These numbers are well off of the experimentally observed peaks at 0.76 and 0.86 eV. Thus,  $\text{Li}_4\text{H}^-$  cannot be responsible for these two peaks. The first and second calculated VDEs for  $\text{LiHLiHLiLi}^-$  with the  $^1\Sigma^+$  ( $1\sigma^2 2\sigma^2 3\sigma^2 4\sigma^0$ ) and  $^3\Sigma^+$  ( $1\sigma^2 2\sigma^2 3\sigma^1 4\sigma^1$ ) final states were found to be 1.39 and 1.83 eV [B3LYP/6-311+G(2df)], and thus  $\text{Li}_4\text{H}_2^-$  cannot explain the experimental features either.

The first calculated VDE for the IV ( $T_d$ ,  $^4A_2$ ) isomer: 0.93 eV (B3LYP/6-311+G(2df)//B3LYP/6-311+G\*), 0.99 eV (CCSD(T)/6-311+G(2df)//CCSD(T)/6-311+G\*), and 1.13 eV (ROVGF/6-311+G(2df), pole-strength is 0.90). This isomer does not appear to be significantly populated under our experimental conditions.

## D. $\text{Li}_5^-$

For the  $\text{Li}_5^-$  cluster, the identification of the most stable geometry becomes nontrivial due to the close energy-spacing of the isomers. Three competitive structures were found to be within 1 kcal/mol of the global minimum. This energy difference is beyond the threshold of our computational accuracy. We therefore conclude that all three clusters, V, VI, and VII (Fig. 2), may be present in the ion beam and contribute to the experimental photoelectron spectrum. This may explain the complexity of the experimental spectrum, which is largely unresolved. Molecular properties of the clusters were published before.<sup>14</sup> Interestingly, cluster VII, which is the third least stable isomer of the anion, is the one whose corresponding neutral exhibits an experimentally confirmed pseudorotation phenomenon.<sup>42–47</sup>

Vertical electron detachment energies of clusters V–VII are collected in Table III. For clusters V and VI, some disagreement can be found between the OVGF results and results obtained in other methods, but for the isomer VII, OVGF performance becomes completely unsatisfactory (Table III). However, the TD-B3LYP and RCCSD(T) results agree well. The first feature in the spectrum, predicted at EBE = 0.64 eV, comes from structure V (Fig. 2), which is a triplet  $D_{3h}$  ( $^3A_1'$ ) species. This VDE corresponds to the loss of an electron from the  $1a_2''$   $\pi$ -MO responsible for  $\pi$ -aromaticity of the cluster (Fig. 3).<sup>14</sup> The threshold of the experimental spectrum begins about there. After the first spectral feature, the theoretically predicted peaks of the three species (V–VII) are grouped around  $\sim 1$ , 2, and 2.6 eV. These are consistent with the EBE range covered by the experimental spectrum. The molecular orbitals corresponding to electron detachments described in Table III are shown in Fig. 3.

## E. $\text{Li}_6^-$

The anionic hexatomic cluster (species VIII, Fig. 2) has only one leading isomer, and all other structures are rendered noncompetitive in terms of their total energies. This is unlike the neutral species, for which four competing isomers were identified in our previous work.<sup>14</sup> For this cluster, all methods used for the interpretation of the photoelectron spectrum agreed on the magnitude of the VDEs (see Table IV and Fig. 1). The first feature in the spectrum corresponds to the detachment of an electron from the singly populated HOMO

TABLE III. Calculated photoelectron spectra of the low-energy isomers of  $\text{Li}_5^-$ .

MO and final state	VDE (eV)		
	TD-B3LYP/6-311+G(2df)// B3LYP/6-311+G*	RCCSD(T)/6-311+G(2df)// CCSD(T)/6-311+G*	U(R)OVGF/6-311+G(2df)// CCSD(T)/6-311+G*
$\text{Li}_5^-$ ( $D_{3h}$ , $^3A_1'$ ) species V			
$1a_2''$ ( $^2A_2''$ )	0.64	...	...
$1e'$ ( $^2E'$ )	0.91	0.94	1.11 (0.86) <sup>a</sup>
$1a_2''$ ( $^4A_2''$ )	1.16	1.15	1.41 (0.79) <sup>b</sup>
$1a_1'$ ( $^4A_1'$ )	2.00	...	3.17 (0.65) <sup>b</sup>
$1a_1'$ ( $^2A_1'$ )	2.81	...	...
$\text{Li}_5^-$ ( $C_{4v}$ , $^1A_1$ ) species VI			
$1e$ ( $^2E$ )	1.02	1.16	1.06 (0.82)
$1a_1$ ( $^2A_1$ )	2.55	...	2.87 (0.63) <sup>b</sup>
$\text{Li}_5^-$ ( $C_{2v}$ , $^1A_1$ ) species VII			
$2a_1$ ( $^2A_1$ )	0.86	0.98	1.99 (0.78) <sup>b</sup>
$1b_2$ ( $^2B_1$ )	1.71	1.78	...
$1a_1$ ( $^2A_1$ )	2.66	...	...

<sup>a</sup>Numbers in parentheses represent pole-strengths.<sup>b</sup>Pole-strength is too low.

( $1a_{2u}$ ), which is a  $\pi$ -MO (Fig. 3). The detachment process leaves the neutral cluster in a singlet state, which is  $\sigma$ -aromatic, as described previously.<sup>14</sup> The second VDE corresponds to the loss of an electron from the doubly degenerated HOMO-1 ( $1e_u$ ), and the process can yield either a singlet or a triplet final state. The deepest valence MO is the HOMO-2 ( $1a_{1g}$ ), and the last two VDEs correspond to the ionization from this MO.

## F. $\text{Li}_7^-$

The heptaatomic anion has two competing isomers (structures IX and X, Fig. 2). The difference of 1.2 kcal/mol in their total energies renders a possibility for both species to be present in the ion beam. Properties of the clusters were reported before.<sup>14</sup> Theoretical VDEs are collected in Table V. One can see that the VDEs of two isomers IX and X can largely explain the experimental spectrum. The first peak in the experimental spectrum (at 1.25 eV) can be assigned as being due to electron detachment from the HOMO ( $1e$ ) of the **X** ( $C_{3v}$ ,  $^1A_1$ ) isomer. This transition was calculated [at B3LYP/6-311+G(2df) and ROVGF/6-311+G(2df)] as occurring with a VDE of 1.20 eV. The first transition of the

IX ( $D_{5h}$ ,  $^1A_1'$ ) isomer may be buried under the tail of the first peak. Its calculated VDE is 0.92 eV using B3LYP/6-311+G(2df) and 0.95 eV using ROVGF/6-311+G(2df) with the pole-strength 0.84. The second experimentally observed peak at 1.55 eV can be assigned to the second VDE of the IX ( $D_{5h}$ ,  $^1A_1'$ ) isomer. Thus VDE was calculated to be 1.66 eV using [B3LYP/6-311+G(2df)] and VDE = 1.67 eV using (ROVGF/6-311+G(2df) with the pole-strength 0.84. The second calculated VDE of the **X** ( $C_{3v}$ ,  $^1A_1$ ) isomer can be assigned to the third highest energy experimental peak at 1.9 eV. This VDE value was predicted to be 1.85 eV using [B3LYP/6-311+G(2df)] and 1.90 eV using (ROVGF/6-311+G(2df) with the pole-strength 0.80.

Overall, the most accurate assignment of the features in the experimental spectrum can be done on the basis of CASSCF-MRCI calculations, which are currently available only for the smallest  $\text{Li}_3^-$  cluster. CCSD(T) also takes into account much of electron correlation and gives quite accurate results most of the time, although it occasionally fails. TD-B3LYP appeared to be the most consistent of all employed methods and gave reliable results throughout the  $\text{Li}_n^-$  series. OVGF does not appear to work well for the studied systems. For all methods based on the Unrestricted

TABLE IV. Calculated photoelectron spectrum of  $\text{Li}_6^-$  ( $D_{4h}$ ,  $^2A_{2u}$ ), species VIII.

MO and final state	VDE, eV			
	TD-B3LYP/6-311+G(2df)// B3LYP/6-311+G*	RCCSD(T)/6-311+G(2df)// CCSD(T)/6-311+G*	UOVGF/6-311+G(2df)// CCSD(T)/6-311+G*	EOM-CCSD(T)/6-311+G(2df)// CCSD(T)/6-311+G*
$1a_{2u}$ ( $^1A_{1g}$ )	1.03	1.00	1.07 (0.84)	1.00
$1e_u$ ( $^3E_g$ )	1.18	1.29	1.31 (0.81)	1.29
$1e_u$ ( $^1E_g$ )	1.60	...	...	1.78
$1a_{1g}$ ( $^3A_{2u}$ )	2.78	...	2.93 (0.81)	...
$1a_{1g}$ ( $^1A_{2u}$ )	3.09	...	...	3.11

<sup>a</sup>Numbers in parentheses represent pole-strengths.

TABLE V. Calculated photoelectron spectra of the low-energy isomers of  $\text{Li}_7^-$ .

MO and final state	VDE (eV)		
	TD-B3LYP/6-311+G(2df)// B3LYP/6-311+G*	RCCSD(T)/6-311+G(2df)// CCSD(T)/6-311+G*	ROVGF/6-311+G(2df)// CCSD(T)/6-311+G*
$\text{Li}_7^-$ ( $D_{5h}$ , $^1A_1'$ ) species IX			
$1a_2''$ ( $^2A_2''$ )	0.92	1.13	0.95 (0.84) <sup>a</sup>
$1e_1'$ ( $^2E_1'$ )	1.66	...	1.67 (0.81)
$1a_1'$ ( $^2A_1'$ )	3.30	...	...
$\text{Li}_7^-$ ( $C_{3v}$ , $^1A_1$ ) species X			
$1e$ ( $^2E$ )	1.20	...	1.20 (0.82)
$2a_1$ ( $^2A_1$ )	1.85	...	1.90 (0.80)

<sup>a</sup>Numbers in parentheses represent pole-strengths.

Hartree–Fock (UHF) wave function, a substantial spin-contamination was found, though results at UCCSD(T) and RCCSD(T) do not differ significantly. Therefore, if a uniform theoretical interpretation of the experimental photoelectron spectrum is desired, TD-B3LYP results should be used, though red shift in calculated VDE should be expected.

## VI. SUMMARY

Small anionic clusters of lithium,  $\text{Li}_x^-$  ( $x = 3-7$ ), have been investigated via a combination of photoelectron spectroscopy and *ab initio* calculations. The structures of the most stable isomers of the anions were identified using the gradient embedded genetic algorithm program. The geometries, vibrational frequencies, and relative energies were further refined at higher levels of theory. Isomers contributing to the experimental spectrum were found. Their electron detachment channels were identified, and vertical detachment energies were computed using a variety of *ab initio* techniques. Photoelectron spectra were successfully interpreted for all systems, except for  $\text{Li}_4^-$ . Furthermore, larger VDEs corresponding to the electron detachment from deeper MOs, which were experimentally inaccessible with the photon energies available in these experiments, were also theoretically determined. This is the first systematic report on small anionic lithium clusters. Until now, these clusters received very limited attention due to the complexity of these systems for both theoretical and experimental characterizations. The work thus contributes to the general understanding of the properties and electronic structure of small lithium cluster anions.

## ACKNOWLEDGMENTS

Theoretical work was supported by the University of California, Los Angeles (A.N.A.) and the National Science Foundation (NSF) under Grant No. CHE-0404937 (A.I.B.). Computer time from the Center for High Performance Computing at Utah State University is gratefully acknowledged. The computational resource, the Uinta cluster supercomputer, was provided through the National Science Foundation under Grant No. CTS-0321170 with matching funds provided by Utah State University. The experimental part of this material (K.H.B.) is based on work supported by the National Science Foundation under Grant No. CHE-0809258.

- <sup>1</sup>J. Simons, *J. Phys. Chem. A* **112**, 6401 (2008).
- <sup>2</sup>A. N. Alexandrova, A. I. Boldyrev, H.-J. Zhai, and L. S. Wang, *Coord. Chem. Rev.* **250**, 2811 (2006).
- <sup>3</sup>H.-J. Zhai and L.-S. Wang, *Chem. Phys. Lett.* **500**, 185 (2010).
- <sup>4</sup>H. W. Sarkas, S. T. Arnold, J. H. Hendricks, V. L. Slager, and K. H. Bowen, *Z. Phys. D: At., Mol. Clusters* **29**, 209 (1994).
- <sup>5</sup>H. W. Sarkas, S. T. Arnold, J. H. Hendricks, V. L. Slager, and K. H. Bowen, *Proc. SPIE* **1858**, 240 (1993).
- <sup>6</sup>H. H. Michels, R. H. Hobbs, and L. A. Wright, *Chem. Phys. Lett.* **118**, 67 (1985).
- <sup>7</sup>K. K. Sunil and K. D. Jordan, *Chem. Phys. Lett.* **104**, 343 (1984).
- <sup>8</sup>H. Partridge, C. W. Bauschlicher, Jr., and E. M. Siegbahn, *Chem. Phys. Lett.* **97**, 198 (1983).
- <sup>9</sup>E. Andersen and J. Simons, *J. Chem. Phys.* **64**, 4548 (1976).
- <sup>10</sup>I. Boustani and J. Koutecky, *J. Chem. Phys.* **88**, 5657 (1988).
- <sup>11</sup>H. W. Sarkas, S. T. Arnold, J. H. Hendricks, and K. H. Bowen, *J. Chem. Phys.* **102**, 2653 (1995).
- <sup>12</sup>B. Temelso and C. D. Sherrill, *J. Chem. Phys.* **122**, 064315 (2005).
- <sup>13</sup>C. W. Bauschlicher, Jr., *Chem. Phys.* **206**, 35 (1996).
- <sup>14</sup>A. N. Alexandrova and A. I. Boldyrev, *J. Chem. Theory Comput.* **1**, 566 (2005).
- <sup>15</sup>J. Ph. Roux and K. H. Bowen, in *Physics and Chemistry of Finite Systems: From Clusters to Crystals*, NATO ASI Series Vol. 1, edited by P. Jena, S. N. Khanna, and B. K. Rao (Kluwer Academic, Dordrecht, 1992), pp. 369–374.
- <sup>16</sup>A. N. Alexandrova, A. I. Boldyrev, Y.-J. Fu, X. Yang, X.-B. Wang, and L.-S. Wang, *J. Chem. Phys.* **121**, 5709 (2004).
- <sup>17</sup>R. G. Parr and W. Yang, *Density-Functional Theory of Atoms and Molecules* (Oxford University Press, Oxford, 1989).
- <sup>18</sup>A. D. Becke, *J. Chem. Phys.* **98**, 5648 (1993).
- <sup>19</sup>J. P. Perdew, J. A. Chevary, S. H. Vosko, K. A. Jackson, M. R. Pederson, D. J. Singh, and C. Fiolhais, *Phys. Rev. B* **46**, 6671 (1992).
- <sup>20</sup>T. Clark, J. Chandrasekhar, C. W. Spitznagel, and P. v. R. Schleyer, *J. Comput. Chem.* **4**, 294 (1983).
- <sup>21</sup>M. J. Frisch, J. A. Pople, and J. S. Binkley, *J. Chem. Phys.* **80**, 3265 (1984).
- <sup>22</sup>J. Cizek, *Adv. Chem. Phys.* **14**, 35 (1969).
- <sup>23</sup>G. D. Purvis III and R. J. Bartlett, *J. Chem. Phys.* **76**, 1910 (1982).
- <sup>24</sup>G. E. Scuseria, C. L. Janssen, and H. F. Schaefer III, *J. Chem. Phys.* **89**, 7382 (1988).
- <sup>25</sup>G. E. Scuseria and H. F. Schaefer III, *J. Chem. Phys.* **90**, 3700 (1989).
- <sup>26</sup>J. A. Pople, M. Head-Gordon, and K. J. A. Raghavachari, *J. Chem. Phys.* **87**, 5968 (1987).
- <sup>27</sup>P. J. Knowles, C. Hampel, and H.-J. Werner, *J. Chem. Phys.* **99**, 5219 (1993).
- <sup>28</sup>K. Raghavachari, G. W. Trucks, J. A. Pople, and M. Head-Gordon, *Chem. Phys. Lett.* **157**, 479 (1989).
- <sup>29</sup>M. E. Casida, C. Jamorski, K. C. Casida, and D. R. Salahub, *J. Chem. Phys.* **108**, 4439 (1998).
- <sup>30</sup>A. D. McLean and G. S. Chandler, *J. Chem. Phys.* **72**, 5639 (1980).
- <sup>31</sup>L. S. Cederbaum, *J. Phys. B* **8**, 290 (1975).
- <sup>32</sup>J. V. Ortiz, *J. Chem. Phys.* **108**, 1008 (1998).
- <sup>33</sup>V. G. Zakrzewski and V. J. Ortiz, *Int. J. Quantum Chem.* **53**, 583 (1995).



- <sup>34</sup>W. von Niessen, J. Shirmer, and L. S. Cederbaum, *Comput. Phys. Rep.* **1**, 57 (1984).
- <sup>35</sup>H.-J. Werner and P. J. Knowles, *J. Chem. Phys.* **89**, 5803 (1988).
- <sup>36</sup>P. J. Knowles and H.-J. Werner, *Chem. Phys. Lett.* **145**, 514 (1988).
- <sup>37</sup>M. J. Frisch, G. W. Trucks, H. B. Schlegel *et al.*, GAUSSIAN 03, Revision C.02, Gaussian, Inc., Wallingford, CT, 2004.
- <sup>38</sup>MOLPRO, a package of *ab initio* programs designed by H.-J. Werner and P. J. Knowles, version 1999, R. D. Amos, A. Bernhardsson, A. Berning *et al.*
- <sup>39</sup>G. Schaftenaar, MOLDEN 3.4, CAOS/CAMM Center, The Netherlands, 1998.
- <sup>40</sup>H. Hotop and W. C. Lineberger, *J. Phys. Chem. Ref. Data* **14**, 731 (1985).
- <sup>41</sup>See supplementary material at <http://dx.doi.org/10.1063/1.3532832> for calculated molecular properties of clusters.
- <sup>42</sup>J. A. Howard, H. A. Joly, R. Jones, P. P. Edwards, R. J. Singer, and D. E. Logan, *Chem. Phys. Lett.* **204**, 128 (1993).
- <sup>43</sup>D. A. Garland and D. M. Lindsay, *J. Chem. Phys.* **78**, 2813 (1983); **80**, 4761 (1984).
- <sup>44</sup>P. Dugourd, D. Rayane, P. Labastie, B. Vezin, J. Chevalere, and M. Broyer, *Chem. Phys. Lett.* **197**, 433 (1992).
- <sup>45</sup>R. Kawai, J. F. Tombrello, and J. H. Weare, *Phys. Rev. A* **49**, 4236 (1994).
- <sup>46</sup>D. A. Gibson and E. A. Carter, *Chem. Phys. Lett.* **271**, 266 (1997).
- <sup>47</sup>R. O. Jones, A. I. Lichtenstein, and J. Hutter, *J. Chem. Phys.* **106**, 4566 (1997).